ARTICLES
PUBLISHED ONLINE: 17 JANUARY 2010 | DOI: 10.1038/NPHYS1508
nature physics

Self-organized adaptation of a simple neural circuit enables complex robot behaviour

Silke Steingrube[1,2], Marc Timme[1,3,4], Florentin Wörgötter[1,4] and Poramate Manoonpong[1,4]*

Controlling sensori-motor systems in higher animals or complex robots is a challenging combinatorial problem, because many sensory signals need to be simultaneously coordinated into a broad behavioural spectrum. To rapidly interact with the environment, this control needs to be fast and adaptive. Present robotic solutions operate with limited autonomy and are mostly restricted to few behavioural patterns. Here we introduce chaos control as a new strategy to generate complex behaviour of an autonomous robot. In the presented system, 18 sensors drive 18 motors by means of a simple neural control circuit, thereby generating 11 basic behavioural patterns (for example, orienting, taxis, self-protection and various gaits) and their combinations. The control signal quickly and reversibly adapts to new situations and also enables learning and synaptic long-term storage of behaviourally useful motor responses. Thus, such neural control provides a powerful yet simple way to self-organize versatile behaviours in autonomous agents with many degrees of freedom.

Specific sensori-motor control and reliable movement generation constitute key prerequisites for goal-directed locomotion and related behaviours in animals as well as in robotic systems. Such systems need to combine information from a multitude of sensor modalities and provide—in real-time—coordinated outputs to many motor units[1]. Already in relatively simple animals, such as a common stick insect or a cockroach, about 10–20 different basic behavioural patterns (several different gaits, climbing, turning, grooming, orienting, obstacle avoidance, attraction, flight, resting and so on) arise from about ten sensor modalities (for example, touch sensors, vision, audition, smell, temperature and vibration sensors) controlling of the order of 100 muscles. Nature apparently has succeeded in creating circuitries specific for such purposes[2–5] and evolution has made it possible to solve the complex combinatorial mapping problem of coordinating a large number of inputs and outputs.

Conventional sensor–motor control methods for technical applications do not yet achieve this proficiency. They typically use for each behavioural output (for example, each walking gait) one specific circuit (control unit), the dynamics of which is determined by several inputs. For example, one may decompose one complex behaviour into a set of simple behaviours each controlled by one unit (ref. 6; 'subsumption architecture'). In this approach of behaviour-based robotics, sensors couple to actuators in parallel. However, conventional methods are difficult to use in self-organizing, widely distributed multi-input multi-output systems[7,8]. For many such systems, neural control seems more appropriate owing to its intrinsically distributed architecture and its capability to integrate new behaviours[9–16].

Here, we address a complex high-dimensional coordination problem using one small neural circuit as a central pattern generator (CPG). The goal is to generate different gaits in an adaptive way and at the same time to coordinate walking with other types of behaviour (such as orienting). To achieve this, the CPG circuit has an intrinsically chaotic dynamics similar to that observed in certain biological CPGs (ref. 17). By means of a newly developed control method we solve the conjoint problem of simultaneously detecting and stabilizing unstable periodic orbits. The method is capable of controlling many different periodic orbits in the same CPG, each of which then leads to one specific activity pattern of the agent. This happens in an autonomous and adaptive way because the states of the sensory inputs of the agent at each moment determine which period to control. As a consequence, the circuit can quickly adapt to different situations. Followed by generic neural postprocessing, this generates a wide range of specific behaviours necessary to appropriately respond to a changing environment. Furthermore, chaotic, uncontrolled dynamics proves behaviourally useful, for example, for self-untrapping from a hole in the ground.

In addition to fast, reactive adaptation based on neural chaos control (required to deal with sudden changes at sensor inputs), the CPG circuit introduced here allows also for learning on longer timescales by synaptic plasticity. This way the system may also permanently accommodate re-occurring correlations between sensor inputs and motor outputs enabling the agent to gradually learn to improve its behaviour.

As a prototypical example we consider a multi-sensor multi-motor control problem of an artificial hexapod to create typical walking patterns emerging in insects[18] as well as several other behaviours. We solve two linked control problems for the artificial hexapod AMOS-WD06 (Fig. 1a,b)[19]: sensor-driven gait selection[20] and sensor-driven orienting behaviour[19,20]. For sensor-driven gait selection, the system receives simultaneous inputs from 13 sensors (see Fig. 1a,c): two light-dependent resistor sensors ($LDR_{1,2}$), six foot-contact sensors ($FC_{1,\ldots,6}$), one gyro sensor (GR), one inclinometer sensor (IM), one current sensor (I), one rear infrared sensor (IR_7) and one auditory-wind detector sensor (AW). They coact to determine the dynamics of a very small, intrinsically chaotic two-neuron module (described below) that serves as a CPG. After postprocessing, the CPG output (Fig. 1d,e) selectively coordinates the action of 18 motors into a multitude of distinct behavioural patterns. Sensor-driven orienting behaviour is controlled by means of four extra infrared sensors ($IR_{1,2,3,4}$) together with the two light-dependent resistor sensors ($LDR_{1,2}$) that generate different types of tropism, for example, obstacle avoidance (negative tropism)

[1]Bernstein Center for Computational Neuroscience, 37073 Göttingen, Germany, [2]Department of Solar Energy, Institute for Solid State Physics, ISFH/University of Hannover, 30167 Hannover, Germany, [3]Network Dynamics Group, Max Planck Institute for Dynamics & Self-Organization, 37073 Göttingen, Germany, [4]Faculty of Physics, University of Göttingen, 37077 Göttingen, Germany. *e-mail: poramate@bccn-goettingen.de.

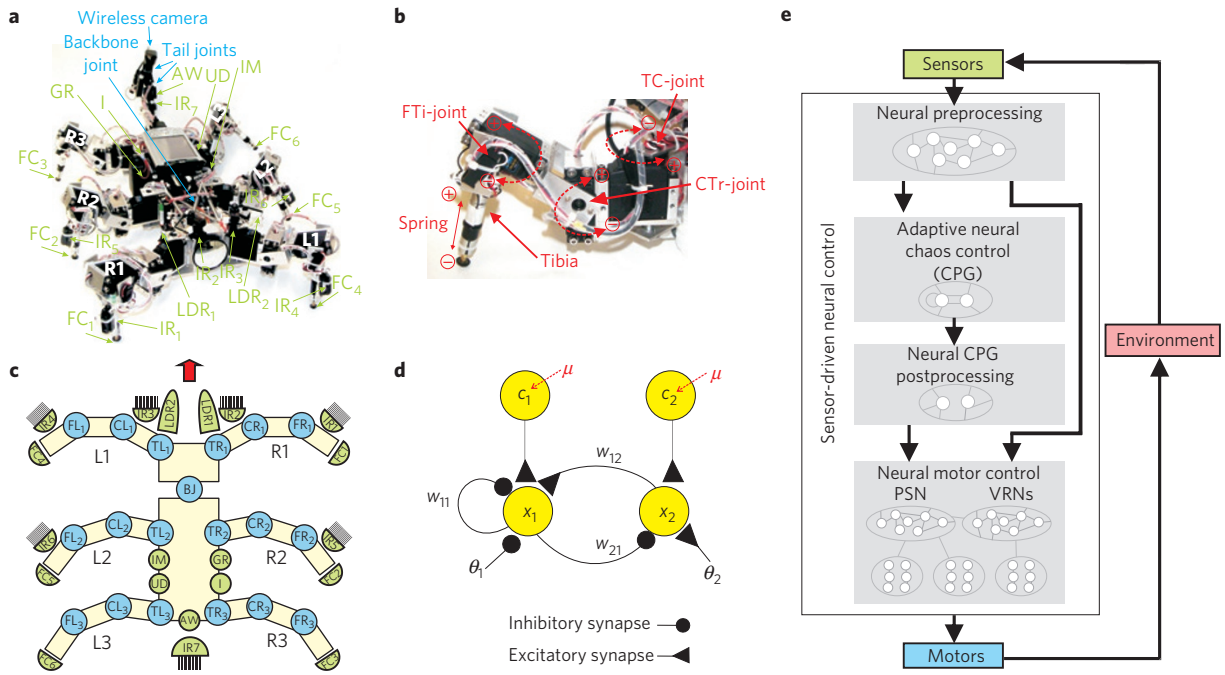

Figure 1 | The six-legged walking machine AMOS-WD06 and the sensor-driven neural control set-up. a, AMOS-WD06 with 20 sensors (green arrows, 18 used here, infrared sensors ($IR_{5,6}$) at the middle legs switched off and not used (but see ref. 19 for their functionality)). **b**, Examples of joints at the right hind leg R3. Red-dashed arrows show directions of forward (+)/backward (−) and up(+)/down(−) movements (see Supplementary Information and Supplementary Fig. S1 for more details). TC-joint refers to the thoraco-coxal joint for forward (+) and backward (−) movements. It corresponds to $TR_{1,2,3}$ and $TL_{1,2,3}$ in **c**. The CTr-joint refers to the coxa-trochanteral joint for elevation (+) and depression (−) of the leg. The hexapod possesses six such joints, three ($CR_{1,2,3}$) on its right and three ($CL_{1,2,3}$) on its left, see **c**. The FTi-joint refers to the femur–tibia joint for extension (+) and flexion (−) of the tibia. This corresponds to $FR_{1,2,3}$ and $FL_{1,2,3}$ in **c**. **c**, Scheme of the hexapod AMOS-WD06 with 20 sensors (green), all 18 leg motor-controlled joints and one backbone joint (blue). **d**, Wiring diagram of the neural control circuit (CPG) consisting of only two neurons with states x_i, $i \in \{1,2\}$ (see equation (1)) and three recurrent synapses of strengths w_{11}, w_{12} and w_{21}. The c_i are self-adapting control signals and μ is the control strength (see equations (2)- (4) and text for details). **e**, The set-up of sensor-driven neural control for stimulus-induced behaviour of AMOS-WD06 (see text for functional description and Supplementary Information and Supplementary Fig. S2 for more details).

and phototaxis (positive tropism) through two extra standard (non-adaptive) neural subnetworks: one phase-switching network (PSN) and two identical modules of a velocity regulating network (VRNs) (see ref. 19 and Supplementary Information for more details). In addition, one upside-down detector sensor (UD) serves to activate a self-protective reflex behaviour when the machine is turned into an upside-down position. In the following, we describe the sensor-driven gait control technique that is based on chaos control. The Supplementary Information describes the technique of controlling sensor-driven orienting behaviour.

To solve the combinatorially hard mapping problem of generating a variety of gait patterns from several simultaneous inputs, we use a simple module of two neurons $i \in \{1,2\}$ (Fig. 1d) as a CPG. The discrete time dynamics of the activity (output) states $x_i(t) \in [0,1]$ of the circuit satisfies

$$x_i(t+1) = \sigma\left(\theta_i + \sum_{j=1}^{2} w_{ij} x_j(t) + c_i^{(p)}(t)\right) \quad \text{for } i \in \{1,2\} \qquad (1)$$

where $\sigma(x) = (1+\exp(-x))^{-1}$ is a sigmoid activation function with biases θ_i and w_{ij} is the synaptic weight from neuron j to i. The control signals $c_i^{(p)}(t)$ act as extra biases that depend only on a single parameter p (the period of the output to be controlled) and are uniquely determined by the sensory inputs (see Table 1). We use synaptic weight and bias parameters (see the Methods section) such that the circuit (equation (1)) shows chaotic dynamics if uncontrolled ($c_i^{(p)}(t) \equiv 0$), see Fig. 2a.

In contrast to previous general methods of controlling chaos[21,22], the method developed and used here both detects and stabilizes periodic orbits at the same time and is implemented in a neural way. The signal $c_i^{(p)}(t)$ is self-adapting and controls the dynamics of the $x_i(t)$ to periodic orbits of period p that are originally unstable and embedded in the chaotic attractor, see refs 21, 23–26. The fact

Table 1 | List of different behaviours achieved given environmental stimuli and conditions.

Environmental stimuli and conditions	Period (p)	Behavioural pattern
Level floor	5	Tetrapod gait
Upward slope	8	Fast wave gait
Rough terrain (hole areas)	8	Fast wave gait
Losing ground contact	Chaos	Self-untrapping
Downward slope	6	Transition or mixture gait
Light stimuli	4	Tripod gait and orienting towards stimuli
Strong light stimuli	1	Resting
Obstacles	4, 5, 6, 8, or 9	Orienting away from stimuli
Turned upside-down	4, 5, 6, 8, or 9	Standing upside-down
Attack of a predator	4	Tripod gait (escape behaviour)
Default	9	Slow wave gait

'Default' means without specific input signals. Note that the mapping between a gait and a period is simply designed by using the fastest useful period, which is $p=4$ ($p=2$ is too fast, $p=3$ does not exist) for the fastest gait and so on, where then $p=9$ is the slowest gait. Period $p=7$ is in shape very similar to $p=6$ and, therefore, it is not used.

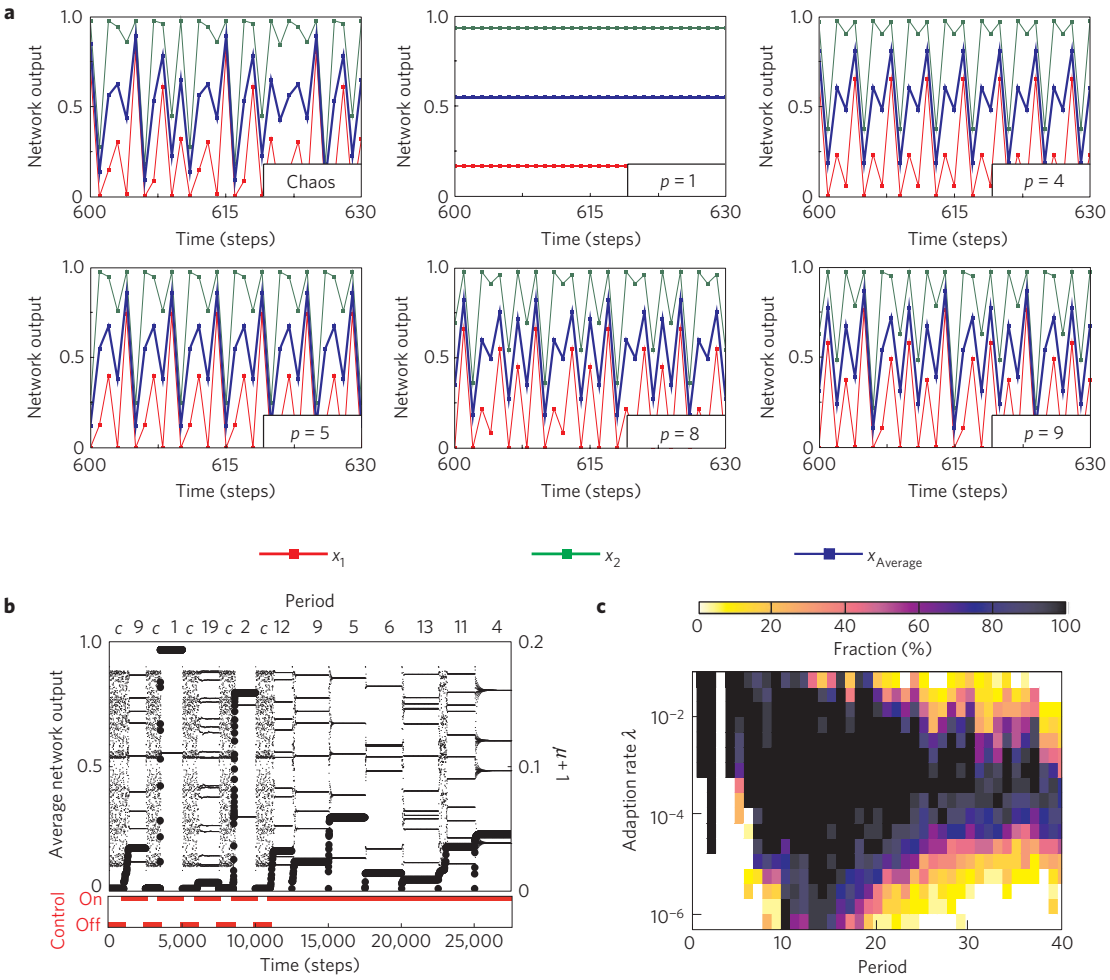

Figure 2 | Control of unstable periodic orbits in the chaotic CPG module. a, CPG dynamics without control (chaotic) and with control to specific periodic orbits $p \in \{1,4,5,8,9\}$. Activity $x_i(t)$ of neurons $i=1$ (red) and $i=2$ (green) are shown for some time window $t \in [600,630]$ along with the average activity $x_{av}=(x_1(t)+x_2(t))/2$ (blue). **b**, Switching between different periodic orbits (period indicated) and chaos (*c*) (adaption rate $\lambda=0.05$). The upper graph shows the average network output x_{av} (thin dots, left axis) and control strength μ (thick dots, right axis) for different target periods *p*. The lower graph shows the time intervals of the control state (on/off). The target period is changed every 2,500 time steps (according to the top legend of **b**), while at the same time the control strength μ is reset to -1. For the first five target periods, control is intermediately switched off for some time intervals such that the system shows chaotic dynamics. For the final seven periods, control remains active such that direct switching between periodic orbits occurs with chaotic dynamics only transiently. With increasing target periods, the control strength tends to adapt to decreasing values μ. **c**, Fraction of correctly controlled periods as a function of adaptation rate and period, colour-coded from black (100% correct) to white (0% correct). Every period is investigated for adaption rates in the range $-\log\lambda \in \{1.2,1.5,\ldots,6.3\}$ for 121 different random initial conditions. An unstable periodic orbit of period three apparently does not exist in the uncontrolled dynamics.

that there is only one CPG makes the control approach conceptually simple, easy to implement and, as shown below, enables the system to self-adapt to new combinations of sensory signals. Note, the combination of these traits and their biological interpretation could not be so easily achieved with any other pattern-generation method (such as, for example, a random-number generator). For a given period *p*, the control signal

$$c_i^{(p)}(t)=\mu^{(p)}(t)\sum_{j=1}^{2}w_{ij}\Delta_j(t) \qquad (2)$$

depends on the differences

$$\Delta_j(t)=x_j(t)-x_j(t-p) \qquad (3)$$

of states separated by one period *p* and is applied every $p+1$ time steps ($\Delta_j(t)=0$ and thus $c_i^{(p)}(t)=0$ at all other times) such that each point of a periodic orbit is controlled sequentially. The control strength $\mu^{(p)}$ adapts according to

$$\mu^{(p)}(t+1)=\mu^{(p)}(t)+\lambda\frac{\Delta_1^2(t)+\Delta_2^2(t)}{p} \qquad (4)$$

with adaption rate λ. The control strength is initialized to $\mu(t_{\text{initial}})=-1$ whenever *p* changes. Here the scaling of the learning increment is heuristically chosen as $1/p$ because a useful learning rate is found to decrease with increasing period *p*.

Figure 2a illustrates that the method successfully generates distinct periodic orbits of different periods, which in turn serve as CPG output patterns. Without control, the CPG signal is chaotic. When being controlled, the CPG dynamics reliably switches to one out of a large variety of periodic outputs (Fig. 2b) and control is successful over a wide range of adaption rates (Fig. 2c). As the chaotic attractors in various dynamical systems contain a large (often infinite) number of unstable periodic orbits[21,23–25], it is in general possible to stabilize many different periodic orbits in

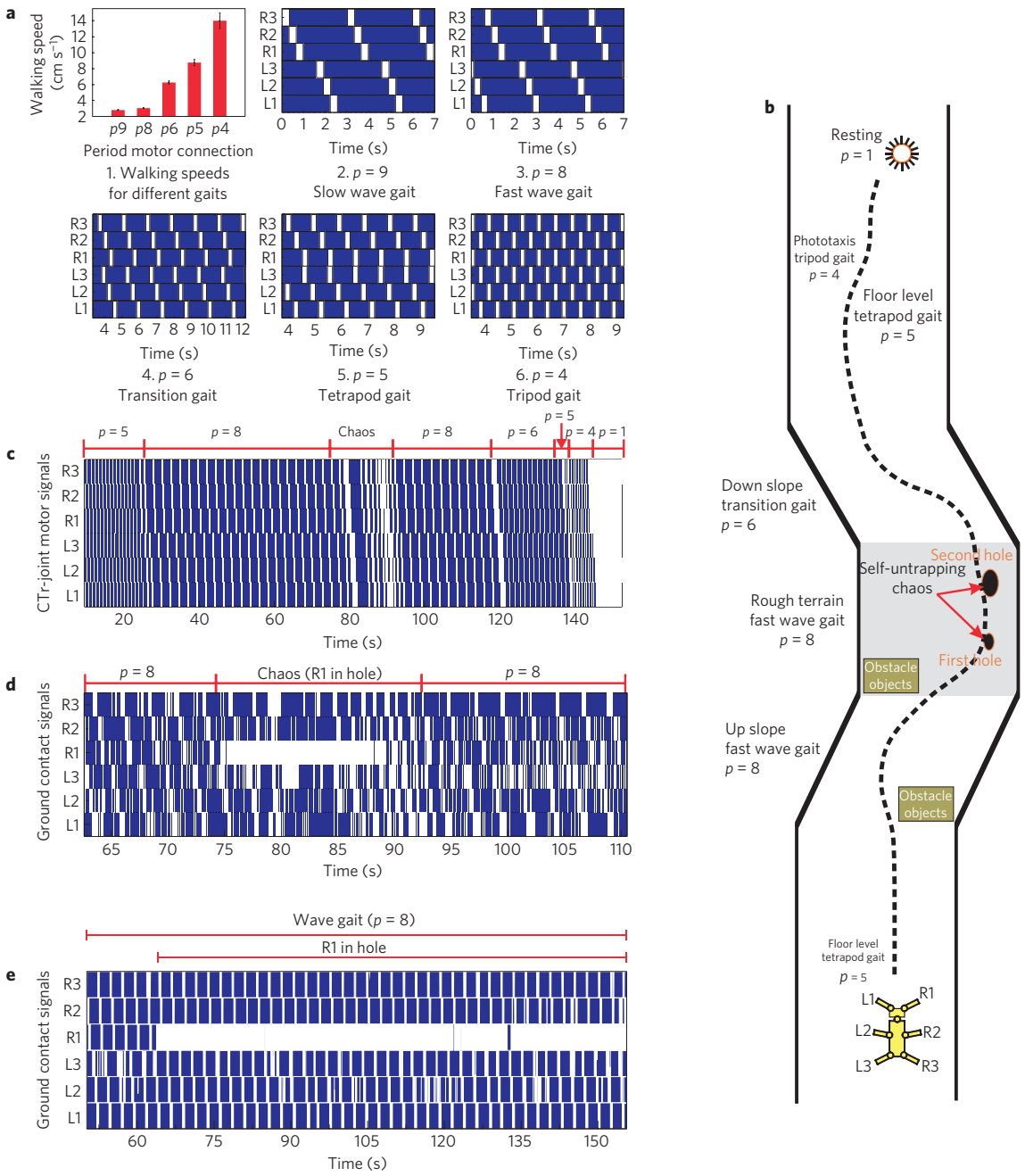

Figure 3 | Chaos-controlled CPG generates sensor-induced behavioural patterns of the hexapod AMOS-WD06. a, Examples of five different gaits (see also Supplementary Fig. S4 and Video S1) observed from the motor signals of the CTr-joints (see Fig. 1b) and walking speeds for these gaits. Throughout the figure, blue areas indicate ground contact or stance phase and white areas refer to no ground contact during swing phase or stepping into a hole during stance phase. **b**, Walking parcour of the hexapod including barriers, obstacle objects, slopes, rough terrain, holes in the ground and light source as phototropic signal (Supplementary Video S2). Behavioural patterns and associated periods of the CPG are indicated. **c**, Gait patterns (expressed as CTr-joint motor signals) observed during walking the entire parcour (Supplementary Video S2). **d**, Foot contact sensor signals at time window 63–112 s, indicating self-untrapping (foothold searching) of right frontal leg (R1) as well as chaotic motion of other legs. **e**, Without chaos, untrapping is not successful, because a periodic gait does not lift the leg out of the hole (compare Supplementary Fig. S6 and Video S4).

essentially any given chaotically oscillating module that may then serve as a CPG. In particular, the functionality is insensitive to variations in the precise module dynamics and a specific type of CPG or a multiple-unit CPG is not required.

Combining the adaptive neural chaos control circuit presented above with standard PSN and VRNs postprocessing (see also Fig. 1e) now enables sensor-driven control of a large repertoire of behaviours. The extracted periodic orbits generate the different gaits (Fig. 3 and Supplementary Video S1), chaotic dynamics actively supports untrapping (see Fig. 3d versus e), and orienting behaviour arises simultaneously, controlled by additional sensory inputs. These features enable the robot to match environmental with behavioural complexity (Supplementary Video S2); in particular, they create specific targeted behaviours such as phototaxis (positive tropism) and obstacle avoidance (negative tropism) (Supplementary Video S3).

Figure 3a–c exemplifies a sequence of eight different behaviours (Supplementary Video S2): standard walking in a tetrapod gait,

up-slope walking in a wave gait, rough-terrain walking in a wave gait, self-untrapping through chaotic motion (Supplementary Fig. S6 and Video S4), down-slope walking in a mixture gait (between wave and tetrapod gait), active phototaxis by fast walking in a tripod gait and resting. As soon as obstacles are detected, the machine moreover performs obstacle avoidance by turning appropriately (Supplementary Fig. S5). Here the irregular chaotic 'ground state' of neural activity (compare with refs 27–31) serves as an intermediate transient state that allows for fast behavioural switching. As soon as the robot gets trapped it actually operates chaotically and exploits chaos for efficient untrapping (Fig. 3d). This demonstrates the capability of the robot to quickly alter its behaviour in response to changing stimulus features from the environment.

The sensor–motor mapping so far was pre-assigned but can also easily be learned (Fig. 4a). All artificial CPGs built so far, including ours, directly map periodic gait patterns (p) to motor patterns m. The most difficult open problem here, thus, is to assure that periods p are selected appropriately given different sensory input conditions s, and hence to learn a suitable mapping $s \rightarrow p$ (Fig. 4a). As the chaos-control strategy uses only one single CPG, the learning problem becomes simple and is solved using only one more single neuron that has plastic synapses. Plasticity is based on standard error minimization learning, which we will describe in general terms next (for details, see the Methods section).

The state variable v of the learning neuron linearly sums many sensor inputs s_k to $v = \sum_k \omega_k s_k$, where ω_k are the synaptic weights to be learned. We randomly assign periods to neuron states in an arbitrary (but fixed) way $v \rightarrow p$ (Fig. 4a) such that different output levels of v result in different gaits. We will now discuss an example where we use a steep and slippery slope on which the agent walks upwards. Of all the agent's sensors, only the inclinometer s_s (slope sensor) will be reliably triggered on the slope. Assuming that its weight changes according to $d\omega_s/dt \sim s_s$, the weight would grow gradually whenever a slope is sensed ($s_s > 0$), leading to increasing v as long as the agent stays on the slope. As the map $v \rightarrow p$ is fixed, the agent checks different values of p one by one trying out different gaits. As a biologically motivated constraint, we now impose in addition that the robot should choose to climb using an energy-saving gait[32]. We hereby define a mechanism that stops learning at that level of v, where such a gait is selected. This is achieved by minimizing an error term e that compares actual energy uptake with the (low) energy uptake of the default gait on flat terrain. If, while climbing, the agent chooses an energy-saving gait, this error will drop to zero. We thus modify our learning rule to rely on the product of error and sensor signal, $d\omega_s/dt \sim s_s \cdot e$, such that learning stops as soon as the error is essentially zero. This happens when ω_s (and, thus, v) have grown to exactly the point where p for the lowest energy gait is selected.

Figure 4b illustrates the dynamics of this learning experiment. Here, the weight ω_s of the slope sensor s_s grows, whereas any uncorrelated synapse, for example ω_g from the gyro sensor s_g, remains unaffected (Fig. 4b). This demonstrates that only the relevant synapses learn. The output v of the learning neuron (Fig. 4a) follows these changes and determines, by means of a threshold mechanism, different values of p (Fig. 4b). As soon as p selects the energy-saving slow wave gait (here $p = 9$), the error e drops to zero, stabilizing synapses and thereby fixing that gait. As the synaptic values remain stored, the next time the hexapod encounters this slope, the inclination sensor will immediately be triggered leading to the same output v and, hence, again to the selection of the slow wave gait (Fig. 4b, right: experiment 2).

In our single-CPG system learning is simplified by the fact that it has to learn only the single map $s \rightarrow p$. Thus, the same neuron v can also be used to learn other sensor–motor mappings. For instance, in a second example of learning (Supplementary Fig. S7 and Video S6)

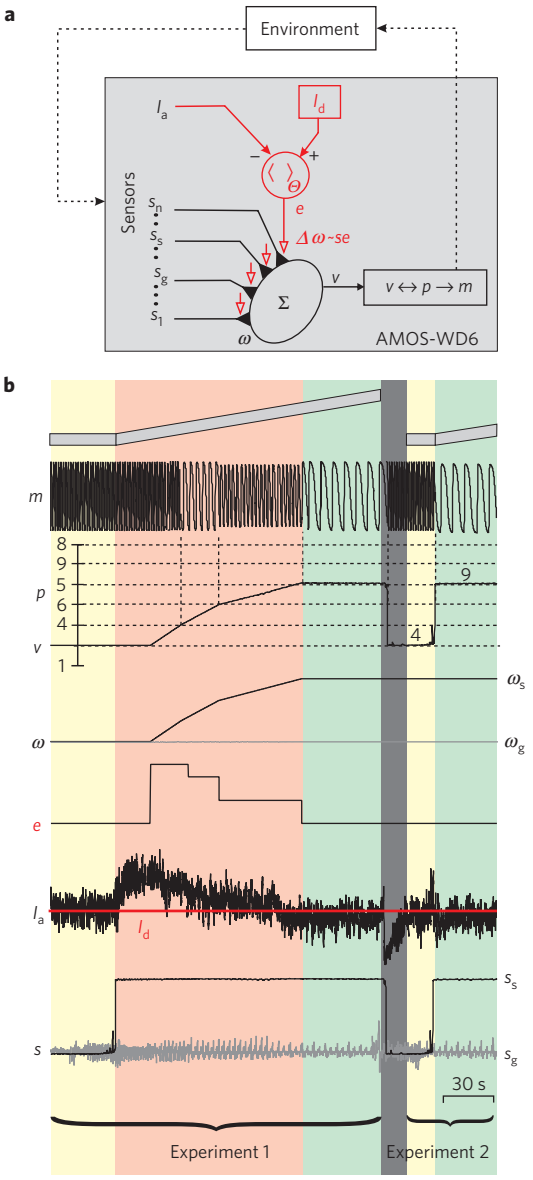

Figure 4 | Learning sensor–motor mappings. a, Wiring diagram for learning. The learning circuit is shown in red. A learning (summation) neuron $\sum$ produces output v from weighted sensor inputs $s_1 \cdots s_n$. The black triangles depict synapses. From output v a gait m is selected using the CPG control signal p, leading to an average actual motor current I_a that depends on the terrain ('Environment'). The actual motor current is compared with the stored default current I_d (red line, for tripod gait on flat terrain) creating an error signal e, which is used for driving synaptic weight changes $\Delta\omega$. The symbol $\langle\,\rangle_\Theta$ denotes a thresholded averaging process (see the Methods section). **b**, Signals during two sequential experiments (see also Supplementary Video S5). Colour code: yellow, flat terrain; red, slope during learning; green, slope after learning; grey, placement of robot back to starting position. m is the motor signal of a TC-joint; s_s is the inclinometer sensor signal; s_g is the gyro sensor signal. In the first experiment the robot on the slope learns to choose the slow wave gait ($p = 9$) that is energy saving and leads to zero error and a drop of I_a. Only the correlated synapse ω_s has grown; the other synapse ω_g remained close to zero. In the second experiment triggering of the inclinometer leads directly to the selection of the slow wave gait without further learning. Note e is computed as an average, leading to a delayed step function. The selection of p from v follows a randomly chosen fixed mapping $v \leftrightarrow p$ shown by the dashed grid lines. Regardless of this mapping, learning will always select the 'zero-error gait' (here the slow wave gait).

we demonstrate how the robot learns to escape from danger by choosing a particularly fast gait.

Thus, single-CPG control based on stabilizing unstable periodic orbits enables self-adaptation of the required sensor–motor mapping $s \leftrightarrow m$. This furthermore underlines a central advantage of the single-CPG approach where pattern generation is robust and learning becomes simple such that extra sensor–motor conjunctions can also be implemented.

We have thus synthesized an integrated system, in which a small, intrinsically chaotic CPG module brings together fast adaptivity in response to changing sensor inputs with long-term synaptic plasticity. Both mechanisms operate on the same network components. The key ingredient here is the time-delayed feedback chaos control that simultaneously detects and stabilizes the dynamics of originally unstable periodic orbits in a biologically inspired, neural way. It is capable of controlling a large number of different periodic orbits of higher periods, a feature not normally achieved in a robust way by standard time-delayed feedback methods[23]. This finally permits implementing learning in an efficient way, namely as a mode selection process at the CPG.

As a consequence, the new strategy enables flexibly configurable control that is readily implemented in hardware, see ref. 19. As it is based on controlling unstable periodic orbits in a generic chaotic system, it does not sensitively depend on the details of the dynamics. For instance, the two-neuron architecture is not necessary and larger chaotic circuits work in a similar way. For the same reason, our strategy may be generalized to integrate other behavioural patterns and can also be applied for controlling different types of kinematic (position controlled) walking machine and behaviour. Transfer to dynamic walking[33] might be possible, too, but would require adding control of extra state variables (for example, forces).

The chosen design is inspired by neural structures found in insects. These combine adaptive CPG function[34] with postprocessing[35,36] similar to the PSN (ref. 37) and VRN (ref. 38) used here. Such individual network components had been used in earlier studies and successfully provided partial solutions to artificial motor-control problems[9–16] indicating that neural control is an efficient way for solving complex sensori-motor control problems. For example, Collins and Richmond[11] have used a network of four coupled nonlinear oscillators as hard-wired CPGs to produce and switch between multiple quadrupedal gait patterns by varying the network's driving signal and by altering internal oscillator parameters. However, embodied control techniques[39] for generating a variety of gait patterns[33,40] jointly with other sensor-driven behaviours[40] in a system with many degrees of freedom are still rare[13,14]. Moreover, these systems either rely on only a smaller number of sensors and motors, or, if more motors are present[9], their coordination forms low-dimensional dynamics such as waves that constrain the motor behaviour to snake- or salamander-like patterns with a uniform gait. Both, small numbers of inputs and outputs and behavioural restrictions reduce the sensor–motor coordination problem substantially.

The capabilities of biological CPGs to generate chaotic as well as periodic behaviour led to the hypothesis that chaos could serve as a ground state for the generation of large behavioural repertoires by the neural activity in these systems (for a review, see ref. 41). The present study now realizes this idea and our chaos-based approach enables a complex combination of walking and orienting behaviour. It simultaneously supports autonomous, self-organized and re-configurable control by adaptively selecting unstable periodic orbits from the chaotic CPG module. Such CPGs might moreover be used for mutual entrainment between neural and mechanical components of a behaving system[42,43]. Adding such features, however, would require further investigations that are more system specific.

Taken together, this work suggests how a chaotic ground state of a simple neuron module may be used in a versatile way for controlling complex robots. It further demonstrates that chaos may also have an active, constructive role for guiding the behaviour of autonomous artificial as well as biological systems. The present study still focuses on reactive motor behaviour. As periodic orbits may be controlled also over longer periods of time, these systems also offer the future possibility of implementing short-term motor memory. Decoupling the centralized control of the CPG from direct sensor inputs would make it more persistent. This opens up the opportunity of implementing behavioural components that make the robotic system capable of navigating and moving with a certain degree of memory-based planning and foresight[44,45].

Methods

Neural control. Sensor-driven neural control for stimulus-induced walking behaviours consists of four neural modules: neural preprocessing, adaptive neural chaos control (CPG), neural CPG postprocessing and neural motor control (Fig. 1e). The controller acts as an artificial perception–action system through a sensori-motor loop. All raw sensory signals go to the neural preprocessing module. It consists of several independent components that eliminate the sensory noise and shape the sensory data (see Supplementary Information for more details). The preprocessed light-dependent resistor ($LDR_{1,2}$), foot contact ($FC_{1,\ldots,6}$), gyro (GR), inclinometer (IM) and rear infrared (IR_7) sensor signals (Fig. 1) are transmitted to the adaptive neural chaos control module. Simultaneously, other preprocessed infrared ($IR_{1,2,3,4}$), upside-down detector (UD) as well as the $LDR_{1,2}$ sensor signals (Fig. 1) are fed to the neural motor control module.

In the adaptive neural chaos control module, a target period for the chaos control is selected according to the incoming sensor signals (see Supplementary Information). This module acts as a CPG where its outputs for different periods determine the resulting gait patterns of the machine (according to Table 1). Here we set the bias values of the CPG circuit as $\theta_1 = -3.4$, $\theta_2 = 3.8$ and the three operating synapses as $w_{11} = -22.0$, $w_{12} = 5.9$, $w_{21} = -6.6$ ($w_{22} = 0.0$), such that it shows chaotic dynamics if uncontrolled ($c_i^{(p)}(t) \equiv 0$), see Fig. 2a. The control strategy is robust against changes of these parameters because it simply relies on the CPG showing chaotic dynamics. It is important to note that chaos on the one hand serves as a ground state of the CPG module; on the other hand it is also functionally used for self-untrapping.

The CPG outputs are passed through the neural CPG postprocessing module for shaping the signal that enters the neural motor control module. The CPG postprocessing module is composed of two single recurrent hysteresis neurons (more details in Supplementary Information) that smooth the signals and two integrator units that transform the discrete smoothed signals to continuous ascending and descending motor signals. Finally, two fixed, non-adaptive subnetworks, PSN and VRNs, of the neural motor control module (Supplementary Fig. S6) regulate and change the CPG signals to expand walking capability allowing turning as well as sidewards and backwards walking. In earlier studies we have shown that the used networks are robust within a wide range of parameters[19]. In fact, it is even possible to use identical VRNs (without change in structure or in parameters) in quadruped robots[46] and transfer the PSN as well as the VRNs to eight-legged machines[19].

Learning. Beyond sensor-driven neural control, we use a modified Widrow–Hoff rule[47] as a learning mechanism to minimize energy consumption as a learning goal (see Supplementary Information for other learning goals). We define the output of the learning neuron as $v = \sum_k \omega_k s_k$ and the rule as $\mathrm{d}\omega_i/\mathrm{d}t = \alpha \cdot e \cdot s_i$, where $\alpha \ll 1$ is the learning rate. The error e is given as $e = \langle I_\mathrm{a} - I_\mathrm{d} \rangle_\Theta$, the symbol $\langle\ \rangle$ denotes averaging over 20 s and we set the error to zero if it is smaller than $\Theta = 0.01$. The variable I_a is the motor current used at present of all motors measured by a sensor (Fig. 1a,c) and I_d is the default current. This is the average current used in a tripod gait on flat terrain.

Walking machine platform. The six-legged walking machine AMOS-WD06 is a biologically inspired hardware platform. It consists of six identical legs where each of them has three joints (three degrees of freedom). All joints are driven by standard servomotors. The walking machine has all in all 20 sensors described in the main section where the potentiometer sensors of the servomotors are not used for sensory feedback to the neural controller. We use a Multi-Servo IO-Board (MBoard) to digitize all sensory input signals and generate a pulse-width-modulated signal to control servomotor position. For the robot walking experiments, the MBoard is connected to a personal digital assistant on which the neural controller is implemented. Electrical power supply is provided by batteries: one 7.4 V lithium polymer 2,200 mAh for all servomotors, two 9 V NiMH 180 mAh for the electronic board (MBoard) and the wireless camera and four 1.2 V NiMH 2,200 mAh for all sensors (see Supplementary Information for more details).

Received 28 April 2009; accepted 11 December 2009; published online 17 January 2010

References

1. Bernstein, N. A. *The Coordination and Regulation of Movements* (Pergamon, 1967).
2. Grillner, S. Biological pattern generation: The cellular and computational logic of networks in motion. *Neuron* **52,** 751–766 (2006).
3. Büschges, A. Sensory control and organization of neural networks mediating coordination of multisegmental organs for locomotion. *J. Neurophysiol.* **93,** 1127–1135 (2005).
4. Pearson, K. G. & Franklin, R. Characteristics of leg movements and patterns of coordination in locusts walking on rough terrain. *Int. J. Robot. Res.* **3,** 101–112 (1984).
5. Ijspeert, A. J. Central pattern generators for locomotion control in animals and robots: A review. *Neural Netw.* **21,** 642–653 (2008).
6. Brooks, R. A. A robust layered control systems for a mobile robot. *IEEE Trans. Robot. Autom.* **2,** 14–23 (1986).
7. Kurazume, R., Yoneda, K. & Hirose, S. Feedforward and feedback dynamic trot gait control for quadruped walking vehicle. *Auton. Robots* **12,** 157–172 (2002).
8. Shkolnik, A. & Tedrake, R. *Proc. IEEE Int. Conf. on Robotics and Automation* 4331–4336 (IEEE Press, 2007).
9. Ijspeert, A. J., Crespi, A., Ryczko, D. & Cabelguen, J. M. From swimming to walking with a salamander robot driven by a spinal cord model. *Science* **315,** 1416–1420 (2007).
10. Kimura, H., Fukuoka, Y. & Cohen, A. H. Adaptive dynamic walking of a quadruped robot on natural ground based on biological concepts. *Int. J. Robot. Res.* **26,** 475–490 (2007).
11. Collins, J. J. & Richmond, S. A. Hard-wired central pattern generators for quadrupedal locomotion. *Biol. Cybern.* **71,** 375–385 (1994).
12. Ayers, J. & Witting, J. Biomimetic approaches to the control of underwater walking machines. *Phil. Trans. R. Soc. A* **365,** 273–295 (2007).
13. Ishiguro, A., Fujii, A. & Eggenberger Hotz, P. Neuromodulated control of bipedal locomotion using a polymorphic CPG circuit. *Adapt. Behav.* **11,** 7–17 (2003).
14. Kuniyoshi, Y. & Sangawa, S. Early motor development from partially ordered neural-body dynamics: Experiments with a cortico-spinal-musculo-skeletal model. *Biol. Cybern.* **95,** 589–605 (2006).
15. Buchli, J., Righetti, L. & Ijspeert, A. J. Engineering entrainment and adaptation in limit cycle systems—from biological inspiration to applications in robotics. *Biol. Cybern.* **95,** 645–664 (2006).
16. Arena, P., Fortuna, L., Frasca, M. & Sicurella, G. An adaptive, self-organizing dynamical system for hierarchical control of bio-inspired locomotion. *IEEE Trans. Syst. Man Cybern. B* **34,** 1823–1837 (2004).
17. Rabinovich, M. I. & Abarbanel, H. D. I. The role of chaos in neural systems. *Neuroscience* **87,** 5–14 (1998).
18. Wilson, D. M. Insect walking. *Annu. Rev. Entomol.* **11,** 103–122 (1966).
19. Manoonpong, P., Pasemann, F. & Wörgötter, F. Sensor-driven neural control for omnidirectional locomotion and versatile reactive behaviours of walking machines. *Robot. Auton. Syst.* **56,** 265–288 (2008).
20. Orlovsky, G. N., Deliagina, T. G. & Grillner, S. *Neuronal Control of Locomotion: From Mollusk to Man* (Oxford Univ. Press, 1999).
21. Ott, E., Grebogi, C. & Yorke, J. A. Controlling chaos. *Phys. Rev. Lett.* **64,** 1196–1199 (1990).
22. Schmelcher, P. & Diakonos, F. K. General approach to the localization of unstable periodic orbits in chaotic systems. *Phys. Rev. E* **57,** 2739–2746 (1998).
23. Schöll, E. & Schuster, H.G. *Handbook of Chaos Control* (Wiley–VCH, 2007).
24. Schuster, H. G. *Deterministic Chaos. An Introduction* (Wiley–VCH, 2005).
25. Schimansky-Geier, L., Fiedler, B., Kurths, J. & Schöll, E. *Analysis and Control of Complex Nonlinear Processes in Physics, Chemistry and Biology* (World Scientific, 2007).
26. Pasemann, F. Complex dynamics and the structure of small neural networks. *Network* **13,** 195–216 (2002).
27. van Vreeswijk, C. & Sompolinsky, H. Chaos in neuronal networks with balanced excitatory and inhibitory activity. *Science* **274,** 1724–1726 (1996).
28. Brunel, N. Dynamics of sparsely connected networks of excitatory and inhibitory spiking neurons. *J. Comput. Neurosci.* **8,** 183–208 (2000).
29. Zillmer, R., Brunel, N. & Hansel, D. Very long transients, irregular firing, and chaotic dynamics in networks of randomly connected inhibitory integrate-and-fire neurons. *Phys. Rev. E* **79,** 031909 (2009).
30. Jahnke, S., Memmesheimer, R.-M. & Timme, M. Stable irregular dynamics in complex neural networks. *Phys. Rev. Lett.* **100,** 048102 (2008).
31. Jahnke, S., Memmesheimer, R.-M. & Timme, M. How chaotic is the balanced state? *Front. Comput. Neurosci.* **3,** 13 (2009).
32. Hoyt, D. F. & Taylor, C. R. Gaits and the energetics of locomotion in horses. *Nature* **292,** 239–240 (1981).
33. Srinivasan, M. & Ruina, A. Computer optimization of a minimal biped model discovers walking and running. *Nature* **439,** 72–75 (2006).
34. Delcomyn, F. Walking robots and the central and peripheral control of locomotion in insects. *Auton. Robots* **7,** 259–270 (1999).
35. Klaassen, B., Linnemann, R., Spenneberg, D. & Kirchner, F. Biomimetic walking robot SCORPION: Control and modelling. *Robot. Auton. Syst.* **41,** 69–76 (2002).
36. Asa, K., Ishimura, K. & Wada, M. Behavior transition between biped and quadruped walking by using bifurcation. *Robot. Auton. Syst.* **57,** 155–160 (2009).
37. Pearson, K. G. & Iles, J. F. Nervous mechanisms underlying intersegmental coordination of leg movements during walking in the cockroach. *J. Exp. Biol.* **58,** 725–744 (1973).
38. Gabriel, J. P. & Büschges, A. Control of stepping velocity in a single insect leg during walking. *Phil. Trans. R. Soc. A* **365,** 251–271 (2007).
39. Pfeifer, R., Lungarella, M. & Iida, F. Self-organization, embodiment, and biologically inspired robotics. *Science* **318,** 1088–1093 (2007).
40. Beer, R. D., Quinn, R. D., Chiel, H. J. & Ritzmann, R. E. Biologically inspired approaches to robotics. *Commun. ACM* **40,** 30–38 (1997).
41. Korn, H. & Faure, P. Is there chaos in the brain? II. Experimental evidence and related models. *C. R. Biol.* **326,** 787–840 (2003).
42. Iida, F. & Pfeifer, R. Sensing through body dynamics. *Robot. Auton. Syst.* **54,** 631–640 (2006).
43. Pitti, A., Lungarella, M. & Kuniyoshi, Y. Exploration of natural dynamics through resonance and chaos. *Proc. 9th Conf. on Intelligent Autonomous Systems* 558–565 (IOS Press, 2006).
44. Wehner, R. Desert ant navigation: How miniature brains solve complex tasks. *J. Comput. Physiol. A* **189,** 579–588 (2003).
45. McVea, D. A. & Pearson, K. G. Long-lasting memories of obstacles guide leg movements in the walking cat. *J. Neurosci.* **26,** 1175–1178 (2007).
46. Manoonpong, P., Pasemann, F. & Roth, H. Modular reactive neurocontrol for biologically-inspired walking machines. *Int. J. Robot. Res.* **26,** 301–331 (2007).
47. Widrow, B. & Hoff, M. E. Adaptive switching circuit. *IRE WESCON Conv. Rec.* **4,** 96–104 (1960).

Acknowledgements

We thank F. Pasemann, T. Geisel, A. Büschges and A. J. Ijspeert for fruitful discussions and acknowledge financial support by the Ministry for Education and Science (BMBF), Germany, through the Bernstein Center for Computational Neuroscience, grant numbers 01GQ0432 (F.W.) and 01GQ0430 (M.T.) as well as by the Max Planck Society (M.T.). F.W. acknowledges financial support by the European Commission 'PACO-PLUS'.

Author contributions

All authors conceived and designed the experiments, contributed materials and analysis tools and analysed the data. S.St. carried out the numerical experiments. P.M. developed the robotic system. P.M. and S.St. carried out the robotic experiments. M.T., F.W. and S.St. worked out the theory. M.T. and F.W. supervised the numerical and robotic experiments. M.T., F.W. and P.M. wrote the manuscript.

Additional information

The authors declare no competing financial interests. Supplementary information accompanies this paper on www.nature.com/naturephysics. Reprints and permissions information is available online at http://npg.nature.com/reprintsandpermissions. Correspondence and requests for materials should be addressed to P.M.